

Pixel-level Scene Understanding in One Token: Visual States Need What-is-Where Composition

Seokmin Lee Yunghee Lee Byeonghyun Pak Byeongju Woo

Agency for Defence Development

{seokminlee, yhl, byeonghyun_pak, woobj903}@add.re.kr

Abstract

For robotic agents operating in dynamic environments, learning visual state representations from streaming video observations is essential for sequential decision making. Recent self-supervised learning methods have shown strong transferability across vision tasks, but they do not explicitly address what a good visual state should encode. We argue that effective visual states must capture *what-is-where* by jointly encoding the semantic identities of scene elements and their spatial locations, enabling reliable detection of subtle dynamics across observations. To this end, we propose **CroBo**, a visual state representation learning framework based on a global-to-local reconstruction objective. Given a reference observation compressed into a compact bottleneck token, CroBo learns to reconstruct heavily masked patches in a local target crop from sparse visible cues, using the global bottleneck token as context. This learning objective encourages the bottleneck token to encode a fine-grained representation of scene-wide semantic entities, including their identities, spatial locations, and configurations. As a result, the learned visual states reveal how scene elements move and interact over time, supporting sequential decision making. We evaluate CroBo on diverse vision-based robot policy learning benchmarks, where it achieves state-of-the-art performance. Reconstruction analyses and perceptual straightness experiments further show that the learned representations preserve pixel-level scene composition and encode *what-moves-where* across observations.

1. Introduction

The world is inherently dynamic: objects move, agents act, and scene configurations continuously evolve over time. For agents to operate reliably in such environments, they must build internal state representations from streams of visual observations and leverage them to support sequential decision making. Learning to encode meaningful, task-

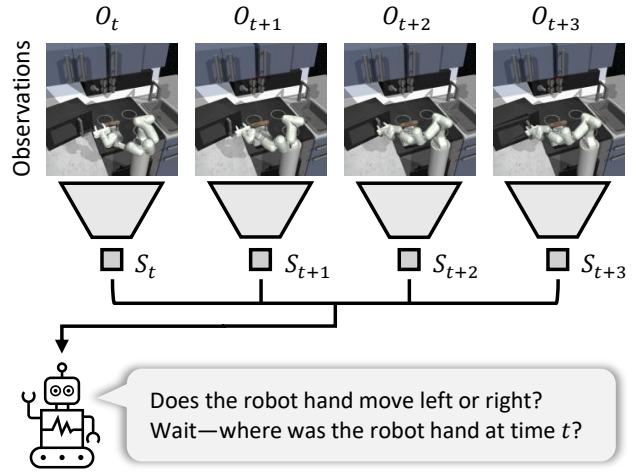


Figure 1. Understanding *what-moves-where* requires knowing *what-is-where*. Robots interact with dynamic environments through compact state representations derived from visual observations. To reason scene dynamics, the robot must understand which objects move and detect how their locations change between observations. This requires each state to capture *what-is-where* information in the scene so that subtle spatial differences between observations can be recognized.

relevant information from raw visual inputs is therefore a central challenge for real-world video applications, including robot learning and world modeling.

Recent studies [5, 7, 8, 16, 17, 28] have demonstrated that self-supervised learning (SSL) methods yield representations with strong transferability to a wide range of downstream vision tasks, such as image classification and semantic segmentation. For robotic agents in particular, however, learning a state representation poses a distinct challenge: the representation must support action by compressing raw observations into a compact visual state while preserving the information essential for decision making [10]. As a recent step in this direction, ToBo [25] introduces a bottleneck token that is trained to reconstruct a heavily masked subsequent frame from a reference observation, using only sparse target patches as hints. This formulation encourages

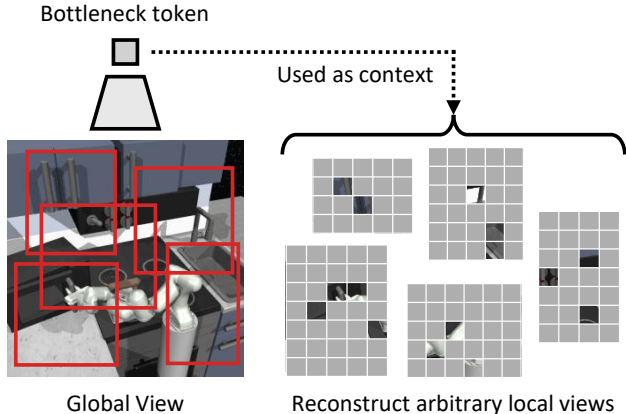


Figure 2. **Learning a visual state that captures pixel-level scene composition.** We present a state representation learning (SRL) method that captures the entire scene composition, including object identities, locations, and their spatial relationship. Conceptually, the global state becomes the bottleneck token that contains the contextual information of the scene. By enforcing reconstruction of arbitrary cropped views from such contextual information, the model is encouraged to encode pixel-level scene composition information in the global state.

the vision encoder to form compact yet temporally aware scene representations. While this approach achieves strong performance on robot learning benchmarks, a fundamental question remains insufficiently addressed: *what should a good visual state representation actually encode?*

We argue that a visual state representation for sequential decision making must capture **what-is-where** by encoding both the semantic identities of scene elements and their precise spatial locations. For example, to recognize that a robot hand has moved from left to right across a sequence of observations, the representation must jointly encode the identity of the hand and its position in the scene; more broadly, it must encode which semantic contents exist in the observation and where they are located, so that even subtle spatial changes can be directly detected. From this perspective, understanding scene dynamics in robotics can be viewed as a form of pixel-level video understanding, where the representation must preserve spatial semantics while remaining sensitive to how they evolve across observations. We posit that this **what-is-where** understanding is the foundation for reasoning about temporal dynamics.

Based on this insight, we propose CroBo, a simple yet effective state representation learning framework designed to capture **what-is-where** visual states. As illustrated in Fig. 2, CroBo builds upon the bottleneck formulation of ToBo [25] and leverages a *global-to-local reconstruction objective* tailored for scene composition learning. Given a reference global observation, the model produces a compact bottleneck serving as a contextual memory of the scene, and is trained to reconstruct an arbitrarily and heavily masked lo-

cal crop using only sparse visible hints from the crop itself. To solve this reconstruction task, the model must infer where the crop originates within the scene and what semantic content should appear there, thereby forcing the representation to preserve fine-grained, pixel-level **what-is-where** information across the full observation. In this way, CroBo learns a compact visual state representation tightly aligned with the requirements of downstream action in dynamic environments.

We validate CroBo through an extensive set of experiments. On vision-based robot policy learning benchmarks, our method achieves state-of-the-art performance. Beyond policy learning results, qualitative reconstruction analyses show that the learned visual state representation indeed captures pixel-level **what-is-where** in the scene. We further show through perceptual straightness experiments that this representation better captures **what-moves-where** across observations. Finally, ablation studies demonstrate individual gains from different objectives, showing the effectiveness of our global-to-local reconstruction approach. In summary, our contributions are threefold:

- We identify that understanding scene dynamics for robot learning requires visual state representations that encode pixel-level **what-is-where**, rather than relying on temporal or patch-level correspondence.
- We introduce CroBo, a self-supervised learning framework that enforces such scene understanding by reconstructing heavily masked local views from a compact representation.
- We show that CroBo achieves state-of-the-art on robot policy learning tasks with representations effectively capturing **what-moves-where**.

2. Method

Claim. Our goal is to learn a compact visual state representation that enables dynamics-aware scene understanding and is transferable to real-world video applications (e.g., robot learning). To this end, we posit that such a representation must capture **what-is-where** scene composition: it should preserve which semantic entities are present in the scene, where they are located, how they relate semantically to each other, and how they are arranged within the overall scene composition. This enables reliable detection of subtle changes and interactions across observations—i.e., understanding **what-moves-where** in the scene.

Overview. We propose CroBo, which learns visual states through a global-to-local reconstruction objective (Fig. 3). The name CroBo reflects our core design: reconstructing an arbitrary **C**ropped local view from a **B**ottleneck token that summarizes the global scene context of the source view. This encourages the visual state representation to capture **what-is-where** in the scene.

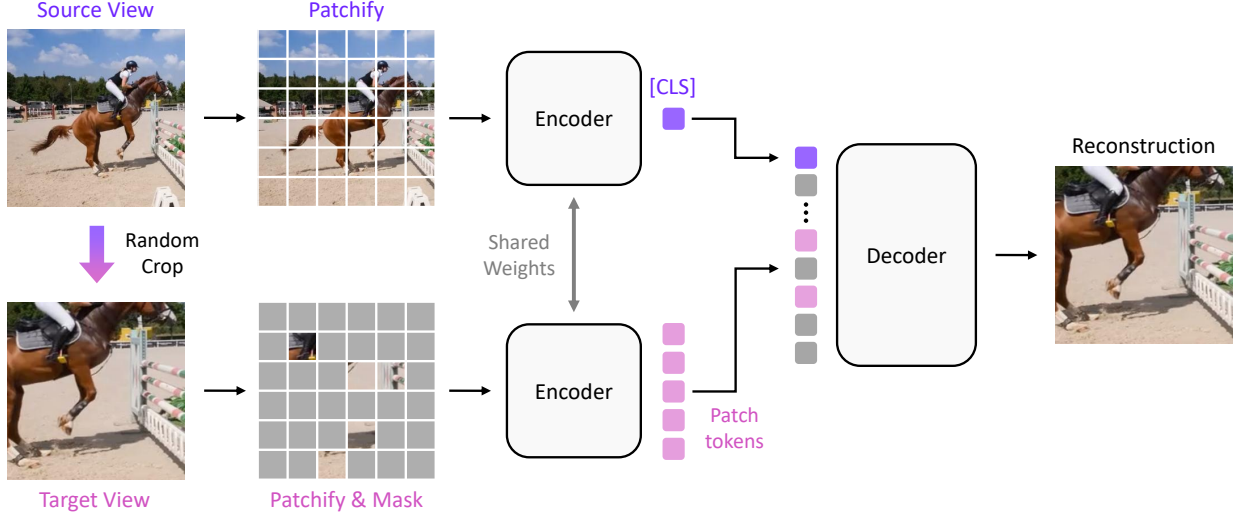


Figure 3. **Overview of CroBo.** Given a global source view \mathbf{x}^g and a local target view \mathbf{x}^l cropped from \mathbf{x}^g , the encoder maps the source view to a single bottleneck token (i.e., [CLS] token) and the target view to a few visible patch tokens under heavy masking (e.g., 90%). The decoder reconstructs the masked target patches from the visible target patch tokens together with source bottleneck token. Because only a few target patches remain visible, the decoder must rely on the bottleneck token to provide the missing scene context, encouraging it to capture fine-grained **what-is-where** scene composition.

Input views. Given a video, we sample a frame and construct a pair of views: a global source view \mathbf{x}^g , obtained by a global crop, and a local target view \mathbf{x}^l , by further cropping \mathbf{x}^g [11]. We patchify each view into N non-overlapping patches, denoted by $\{\mathbf{x}_i^g\}_{i=1}^N$ and $\{\mathbf{x}_i^l\}_{i=1}^N$. Note that the source view contains all the information in the target view, as \mathbf{x}^l is spatially contained within \mathbf{x}^g .

Siamese encoder and Masking. We encode both the source and target views using a shared-weight Siamese encoder [3, 15]. The source view \mathbf{x}^g is processed without masking, whereas the target view \mathbf{x}^l is masked with a high masking ratio r (e.g., 90%) before being fed into the encoder. We intentionally apply a higher masking ratio than MAE [17] (75%) to prevent the target view from being reconstructed solely from the visible tokens. Let $\mathcal{M} \subset \{1, \dots, N\}$ denote the set of masked patch indices, where $|\mathcal{M}| = \lfloor rN \rfloor$, and let $\mathcal{M}^c = \{1, \dots, N\} \setminus \mathcal{M}$ denote the set of visible patch indices. The source and target views are then encoded as

$$\mathbf{z}_{\text{cls}}^g, \{\mathbf{z}_i^g\}_{i=1}^N = \text{Encoder}(\{\mathbf{x}_i^g\}_{i=1}^N), \quad (1)$$

$$\mathbf{z}_{\text{cls}}^l, \{\mathbf{z}_i^l\}_{i \in \mathcal{M}^c} = \text{Encoder}(\{\mathbf{x}_i^l\}_{i \in \mathcal{M}^c}). \quad (2)$$

Here, $\mathbf{z}_{\text{cls}}^g$ and $\mathbf{z}_{\text{cls}}^l$ denote the [CLS] tokens of the source and target views, respectively, while $\{\mathbf{z}_i^g\}_{i=1}^N$ and $\{\mathbf{z}_i^l\}_{i \in \mathcal{M}^c}$ denote the corresponding patch tokens.

Decoder. We reconstruct the masked target view using a Transformer decoder consisting of stacked self-attention and MLP blocks. Specifically, we first restore the full target token sequence by inserting a learnable mask token at the

masked positions and adding positional embeddings. The source [CLS] token $\mathbf{z}_{\text{cls}}^g$, which serves as a single bottleneck token for the source view, is then concatenated with the restored target patch tokens and fed into the decoder. The masked target patches are reconstructed as

$$\{\hat{\mathbf{x}}_i^l\}_{i=1}^N = \text{Decoder}([\mathbf{z}_{\text{cls}}^g; \{\tilde{\mathbf{z}}_i^l\}_{i=1}^N]), \quad (3)$$

where $\{\tilde{\mathbf{z}}_i^l\}_{i=1}^N$ is the restored target token sequence. In this design, the decoder must infer the missing target content from two complementary signals: sparse local hints from the visible target patches and global scene context carried by the bottleneck token $\mathbf{z}_{\text{cls}}^g$. As a result, $\mathbf{z}_{\text{cls}}^g$ is encouraged to preserve the information not only which semantic objects are present in the scene but also where each of them is located, so that the masked target region can be reconstructed faithfully.

Objective. We train the encoder and decoder jointly by minimizing the mean squared error over the masked target patches, using normalized pixel targets [17]. The loss is defined as

$$\mathcal{L} = \frac{1}{|\mathcal{M}|} \sum_{i \in \mathcal{M}} \|\hat{\mathbf{x}}_i^l - \mathbf{x}_i^l\|_2^2. \quad (4)$$

Why train on video datasets? CroBo constructs both views from a single frame and therefore does not require multiple video frames for pre-training. We nevertheless train CroBo on a video dataset to ensure fair comparison with prior works [11, 15, 22, 25].

Table 1. **Experimental results on vision-based robot policy learning.** We evaluate imitation learning performance on Franka Kitchen [14] and DeepMind Control Suite (DMC) [30]. The agents are trained on frozen visual representations extracted from a ViT-S/16 encoder pre-trained on the Kinetics-400 [24], except for DINOv2. Success rates (%) are reported for Franka Kitchen and normalized scores are reported for DMC. The best results are **bold**, second-best are underlined. † denotes numbers taken from [22]. We report the gains of our method over the previous state-of-the-art method.

Model	Franka Kitchen					DeepMind Control Suite			
	Knob on	Light on	Sdoor open	Ldoor open	Micro open	walker/stand	walker/walk	reacher/easy	finger/spin
MAE†	12.0±3.3	24.3±4.2	71.5±4.3	12.8±3.9	10.0±2.8	-	-	-	-
DINO†	27.0±3.2	44.3±6.5	77.0±5.0	16.5±2.5	28.5±4.8	-	-	-	-
DINOv2	25.0±1.4	46.6±5.8	87.8±2.7	17.6±2.4	21.8±3.5	81.2±3.7	38.2±2.1	<u>87.6±3.8</u>	67.4±0.8
SiamMAE†	16.8±4.4	36.5±7.0	68.0±7.9	17.3±3.7	13.5±4.8	-	-	-	-
CropMAE	33.0±3.1	65.0±5.1	89.6±2.1	22.6±2.2	25.0±2.9	59.9±4.5	33.8±3.7	75.4±2.8	69.9±0.8
RSP	33.0±2.5	44.8±9.3	89.6±3.8	25.8±4.1	33.4±1.7	77.3±2.5	64.6±5.0	63.1±3.6	68.5±0.7
ToBo	58.4±5.1	<u>80.6±4.8</u>	<u>98.4±1.1</u>	44.2±10.0	<u>51.2±6.1</u>	87.0±3.0	<u>77.7±4.4</u>	87.5±3.3	<u>69.6±0.8</u>
CroBo (Ours)	65.6±3.7	87.6±2.2	99.4±1.0	<u>41.2±5.6</u>	64.8±4.4	92.0±1.4	80.8±3.0	95.8±2.1	69.9±0.7
△ prev. SOTA	+7.2	+7.0	+1.0	-3.0	+13.6	+5.0	+3.1	+8.3	+0.0

3. Experiments

We first demonstrate the effectiveness of CroBo on vision-based robot policy learning benchmarks, including robotic manipulation and locomotion (Sec. 3.2). We then analyze the learned representation to better understand its properties. **1)** Through reconstruction visualizations, we examine how well the state token captures **what-is-where** scene composition (Sec. 3.3). **2)** Through perceptual straightness in video, we analyze how this representation supports **what-moves-where** understanding across observations (Sec. 3.4).

3.1. Implementation details

Pre-training. For a fair comparison, we follow the pre-training setup of RSP [22]. Specifically, we use ViT-S/16 [9] and pre-train on the Kinetics-400 dataset [24] for 400 epochs with a repeated sampling value of 2 [12, 20]. For spatial views x^g and x^l , we adopt the global-to-local cropping configuration of [11]. We apply a masking ratio of 90% to the target view x^l . The decoder consists of 8 layers with an embedding dimension of 512. We optimize the model using AdamW [26] with a batch size of 1536.

Competitors. We compare our method with (1) standard self-supervised learning (SSL) methods, including MAE [17], DINO [5], and DINOv2 [28]. We also compare with (2) SSL methods for dynamic scenes, including SiamMAE [15], CropMAE [11], RSP [22], and ToBo [25].

3.2. Vision-based Robot Learning

In this section, we evaluate the proposed method on two vision-based policy learning benchmarks, Franka Kitchen and the DeepMind Control Suite (DMC), covering robotic manipulation and locomotion tasks in simulated environments.

Evaluation setup. Across both benchmarks, we freeze the pre-trained visual backbone and train an MLP policy head via behavior cloning using a mean squared error (MSE) loss. A batch normalization layer is applied to the policy input, and results are reported with 95% confidence intervals over multiple independent runs.

Franka Kitchen. Following the experimental protocol of RSP [22], we evaluate our method and competing baselines on five tasks from the Franka Kitchen benchmark [14]. The policy input is formed by concatenating the visual embedding with the robot proprioceptive observations, and the policy head is implemented as an MLP with two hidden layers of 256 units each. Visual observations are captured from left and right camera viewpoints as 224×224 RGB images. The policy is trained with a batch size of 32 and 25 expert demonstrations for 20,000 gradient steps, with online evaluation in simulation performed every 1,000 training steps. We report the mean peak success rate, averaged over 10 independent runs across five random seeds and two camera viewpoints.

DeepMind Control Suite. We evaluate our method and competing baselines on four tasks from the DeepMind Control Suite (DMC) [30], spanning both manipulation and locomotion tasks. The policy input is formed solely from the visual embedding, without proprioceptive observations, and the policy head is implemented as an MLP with three hidden layers of 256 units each. Visual observations are captured as 224×224 RGB images with a history window of three consecutive frames. The policy is trained with a batch size of 256 and 100 expert demonstrations for 100 epochs, with online evaluation performed every 5 epochs. We report the mean peak normalized score, averaged over 10 independent runs across 10 random seeds.

Table 2. Scalability of our method on Franka Kitchen [14]. Success rates (%) are reported for ViT-S/16, ViT-B/16, and ViT-L/16 backbones pre-trained on Kinetics-400 [24] for 100 epochs. While ViT-S results are provided for CroBo, ViT-B and ViT-L scales include comparisons with SiamMAE [15], RSP [22], and ToBo [25]. Δ denotes the performance margin relative to the best-performing baseline in each scale. Best results are in **bold** and second best are underlined. CroBo results are averaged over 10 trials, while baseline results and those marked with \dagger are from [25].

Arch.	Method	Knob1 on	Light on	Sdoor open	Ldoor open	Micro open	5-task Avg.
ViT-S/16	CroBo (Ours)	57.6 \pm 8.1	81.6 \pm 2.1	98.6 \pm 1.4	36.8 \pm 3.8	50.4 \pm 5.8	65.0 \pm 4.2
ViT-B/16	SiamMAE \dagger	18.0 \pm 2.0	34.0 \pm 2.0	80.7 \pm 3.1	18.7 \pm 1.2	19.3 \pm 6.1	34.1 \pm 2.9
	RSP \dagger	24.7 \pm 3.1	51.7 \pm 9.1	87.3 \pm 2.3	23.3 \pm 7.6	26.7 \pm 2.3	42.7 \pm 4.9
	ToBo \dagger	46.7 \pm 6.4	78.7 \pm 7.6	95.3 \pm 1.2	47.3 \pm 5.0	37.3 \pm 4.6	61.1 \pm 5.0
	CroBo (Ours)	64.4 \pm 2.4	86.2 \pm 3.7	98.0 \pm 1.0	41.0 \pm 6.6	62.8 \pm 3.4	70.5 \pm 3.4
	Δ prev. SOTA	+17.7	+7.5	+2.7	-6.3	+25.5	+9.4
ViT-L/16	SiamMAE \dagger	20.7 \pm 3.1	34.0 \pm 4.0	76.0 \pm 2.0	12.7 \pm 6.4	22.0 \pm 0.0	33.1 \pm 3.1
	RSP \dagger	26.7 \pm 2.3	48.0 \pm 2.0	88.0 \pm 2.0	22.7 \pm 8.3	23.3 \pm 4.2	41.7 \pm 3.8
	ToBo \dagger	54.7 \pm 5.0	75.3 \pm 4.2	94.0 \pm 3.5	50.0 \pm 2.0	42.7 \pm 6.1	63.3 \pm 4.2
	CroBo (Ours)	62.4 \pm 3.1	85.8 \pm 3.7	98.6 \pm 1.0	42.8 \pm 5.3	66.0 \pm 5.0	71.1 \pm 3.6
	Δ prev. SOTA	+7.7	+10.5	+4.6	-7.2	+23.3	+7.8

Reproducibility. Benchmark performance in vision-based robot learning can exhibit substantial variance across runs due to random seed sensitivity and environment version discrepancies. While prior work commonly reports results averaged over 5 trials (e.g., RSP [22], ToBo [25]), we evaluate each method over 10 trials within a unified environment to facilitate more reliable comparisons. For methods with publicly available checkpoints (DINOv2 [28], CropMAE [11], RSP [22], and ToBo [25]), we re-evaluate directly using the released weights. For MAE [17], DINO [5], and SiamMAE [15], whose Kinetics-400 [24] pretrained checkpoints are not publicly available, we adopt the results reported in RSP [22].

Result. Tab. 1 reports the performance of our method and prior self-supervised learning methods on the Franka Kitchen [14] and the DeepMind Control Suite benchmarks [30]. Overall, CroBo consistently outperforms existing approaches across most tasks. On the Franka Kitchen benchmark, CroBo achieves the best performance on four out of five tasks, substantially improving over the previous state-of-the-art. In particular, it yields large gains on Micro open (+13.6%), Knob on (+7.2%), and Light on (+7.0%). On the DeepMind Control Suite, our method similarly establishes new best results across several tasks, with the most notable improvements on reacher/easy (+8.3%), walker/stand (+5.0%), and walker/walk (+3.1%). Importantly, these improvements are observed across both robotic manipulation and locomotion tasks. This suggests that the representations learned by CroBo capture visual features that generalize across diverse embodied control problems, rather than being tailored to a specific domain.

Scaling behavior. To evaluate the scalability of our method across different model capacities, we benchmark CroBo against baselines using ViT-B/16 and ViT-L/16 backbones, and report ViT-S/16 results for CroBo. All models are pre-trained on Kinetics-400 [24] for 100 epochs and evaluated on Franka Kitchen [14]. As shown in Tab. 2, CroBo consistently outperforms SiamMAE [15], RSP [22], and ToBo [25] across all architecture scales. The base and large variants achieve 5-task average success rates of 70.5% and 71.1%, respectively, surpassing the prior state of the art by substantial margins of +9.4% and +7.8%. Remarkably, even our smallest backbone (ViT-S/16) attains a 65.0% average success rate, outperforming all baselines that use the much larger ViT-L/16 architecture. These results demonstrate that the performance gains of CroBo are not due to model scale. Instead, they reflect a fundamentally stronger representation that generalizes robustly across the full spectrum of model capacities.

3.3. Qualitative Analysis

In this section, we examine how well the bottleneck token captures **what-is-where** scene composition through reconstruction visualizations.

Target datasets. We visualize image reconstructions on CLEVR [23], DAVIS [29], and Franka Kitchen [14]. CLEVR provides synthetic scenes with simple spatial layouts and clearly defined object attributes (e.g., color, shape and materials), making it well-suited for evaluating **what-is-where** scene composition. DAVIS extends the analysis to natural video scenes with diverse semantic objects and appearance variations, whereas Franka Kitchen provides complex robotic manipulation scenes.

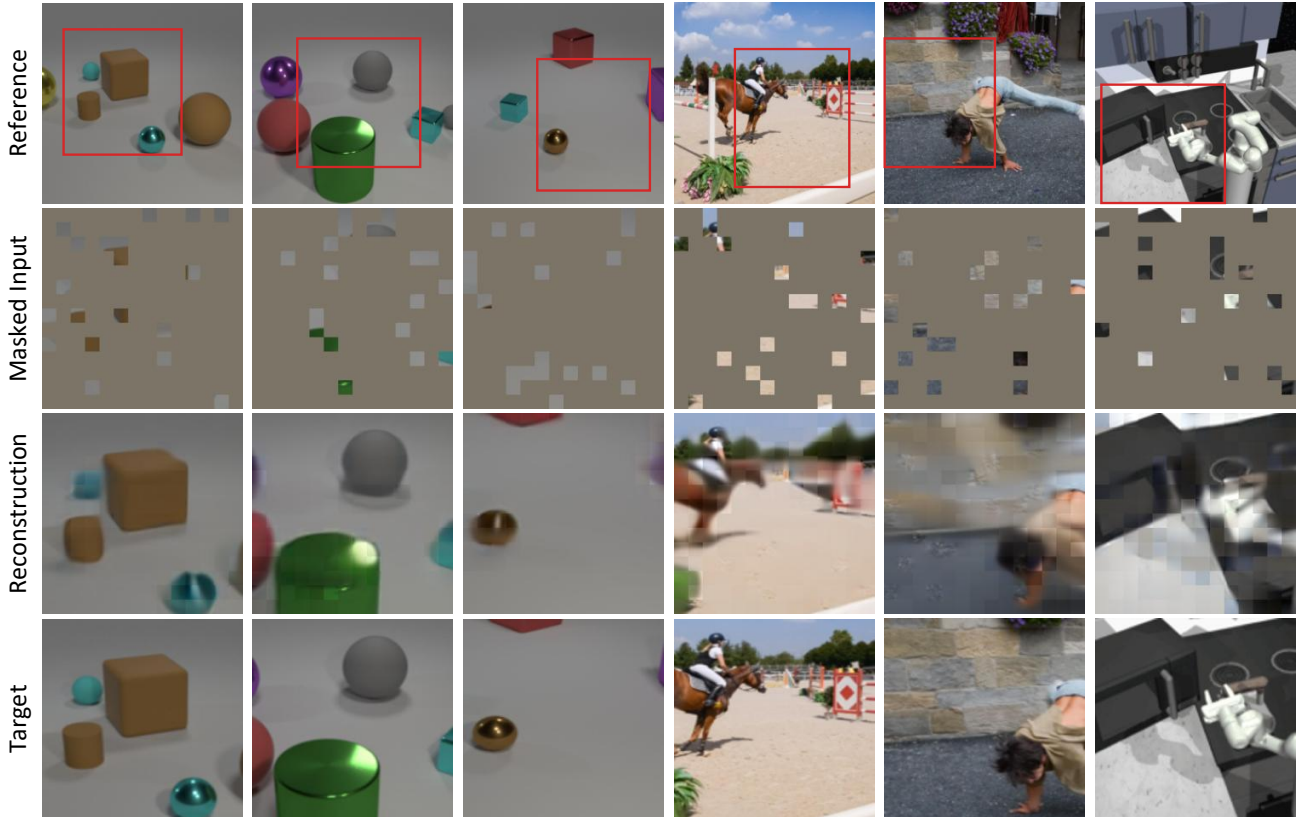


Figure 4. **Reconstruction of CroBo.** We visualize image reconstructions on CLEVR [23] (columns 1-3), DAVIS [29] (columns 4-5), and Franka Kitchen [14] (column 6). Using the bottleneck token of the source view as context, CroBo reconstructs a highly masked (90%) target view cropped from the source view. The results show that CroBo representations effectively capture the global scene structure, including object identities, locations, and their spatial relationships.

Analysis. We follow the same reconstruction setup used during training (Fig. 4). A target view is obtained by randomly cropping the reference image. We then mask 90% of the target patches and reconstruct the view from the visible patches using the bottleneck token as context. The first example shows that the bottleneck token preserves object attributes together with spatial locations and relationships: the two cyan spheres are correctly reconstructed even though they are completely invisible in the masked input. The second example shows that the representation captures fine-grained object and scene details, such as metallic material and shadows. The fourth example shows that the bottleneck token retains the person-horse relationship in the scene: from only a few visible person parts, the model plausibly reconstructs both the horse shape and person’s pose. This suggests that the bottleneck token captures how objects are semantically arranged in the scene. The last example helps explain the strong robotic performance of CroBo. The representation consistently preserves **what-is-where** scene composition even in complex scenes, which is critical for localizing affordance-bearing objects during manipulation.

Additional results are provided in the supplementary material.

3.4. Perceptual Straightness in Video

In this section, we analyze the temporal geometry of representations of our dynamics-aware SSL model. Specifically, we investigate whether representations evolve smoothly over time when processing natural videos using the concept of *perceptual straightening* [18, 19]. In particular, we measure the local curvature of representation trajectories induced by sequential video frames and compare them across models.

Perceptual straightness. Perceptual straightness is the property of perceptual representations in which the visual system transforms inputs to follow a straight path in the representation space. Since observations vary in a complex and highly nonlinear way in the pixel space, it is infeasible to make meaningful predictions from raw observations [27]. Therefore effective video understanding systems [1, 18] compress raw observations into a visual state that has a locally straight temporal trajectory. This makes predicting

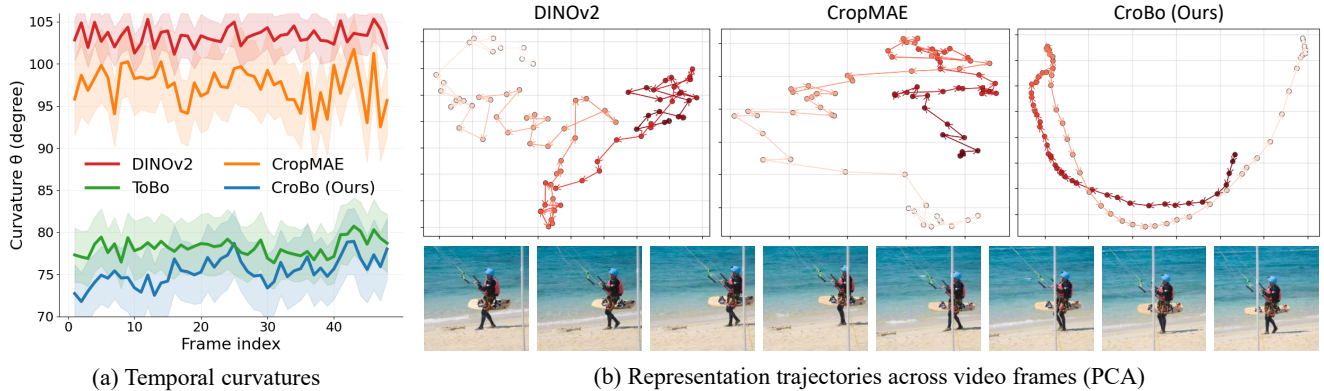


Figure 5. **Perceptual straightness of representation dynamics in video.** (a) Local curvature of representation trajectories measured on DAVIS videos. Curvature is computed as the angle between consecutive representation differences, averaged across videos. Lower curvature indicates smoother temporal dynamics. CroBo consistently exhibits lower curvature than prior models such as DINOv2 and CropMAE, suggesting more temporally coherent representations that better preserve **what-moves-where** across frames. (b) Representation trajectories across video frames visualized using PCA. Each point corresponds to the representation of a frame, and colors indicate temporal progression. CroBo produces smooth and locally linear trajectories that follow the natural evolution of the scene, whereas DINOv2 and CropMAE produce irregular and tangled trajectories.

future states possible via linear extrapolation.

Measuring perceptual straightness. Local curvature is the main metric to assess the perceptual straightness of representations [18, 21]. Formally, let $z_t = f_\theta(x_t)$ denote the representation of frame x_t produced by an encoder f_θ . The temporal trajectory of a video in representation space is given by the sequence $\{z_t\}_{t=1}^T$. We measure the local curvature using the angle between consecutive difference vectors $\Delta z_t = z_{t+1} - z_t$ and $\Delta z_{t+1} = z_{t+2} - z_{t+1}$ as

$$\theta_t = \arccos \left(\frac{\Delta z_t \cdot \Delta z_{t+1}}{\|\Delta z_t\|_2 \cdot \|\Delta z_{t+1}\|_2} \right). \quad (5)$$

Lower curvature values indicate that representation trajectories evolve more linearly over time, suggesting temporally consistent features that effectively encode **what-moves-where**. In other words, a model understanding smooth motion will produce a smooth trajectory of representations [18]. We evaluate the perceptual straightness of representations generated by models both quantitatively and qualitatively to demonstrate the effectiveness of our approach.

Quantitative comparison. We measure local curvature on videos of the DAVIS validation set. For each video containing at least 50 frames, we compute the trajectory and the local curvature for the first 50 frames and plot the average local curvature at Fig. 5(a). CroBo achieves an average curvature of 75.4° , compared to 103.28° of DINOv2. The lower curvature values signal that representations of our dynamics-aware SSL model follows a locally linear path. This result suggests that our model is able to capture subtle temporal differences between adjacent frames and maintain a coherent representation of **what-moves-where**.

An example trajectory. As an intuitive example, we compute representations of frames from the kite-walk video in the DAVIS dataset [29]. Then we compute two principal components of the trajectory via PCA and plot it at Fig. 5(b) following [1]. While DINOv2 and CropMAE generated highly jagged trajectories, CroBo produced a smooth trajectory, demonstrating a consistent understanding of **what-moves-where**. The trajectory is also compliant to the contents of the video; while the person moves right and then left in the video, the representation also moves back and forth in the first principal component.

3.5. Ablation on Target View Construction

In this section, we compare our *global-to-local* relationship with another promising *source-to-target* relationship for visual state representation learning (SRL).

Preliminary. To learn visual correspondences between two views, SiamMAE [15] constructs a *current-to-future* relationship, by randomly sampling two frames from a video. In contrast, CropMAE [11] constructs a *global-to-local* relationship, by generating the target view through cropping the source view. In our ablation study, we denote these two formulations as **Time** and **Crop**, respectively. Our proposed method corresponds to Crop.

Time vs Crop. We compare the two source-to-target formulations, Time and Crop, by pre-training ViT-S/16 on Kinetics-400 for 100 epochs and evaluating on Franka Kitchen. As shown in Tab. 3, Crop consistently outperforms Time across all five tasks. This result is somewhat surprising, since Crop does not use temporal cues, yet achieves better transfer on dynamic downstream tasks that require tem-

Table 3. Ablation on the construction of the target view. Models are pre-trained on Kinetics-400 for 100 epochs and evaluated on Franka Kitchen (success rate %). “Time” uses a future frame at time $t + k$ as the target view. “Crop” uses a cropped local region as the target view. Our method is highlighted in gray .

Time	Crop	Knob1	Light	Sdoor	Ldoor	Micro
✓		44.4	67.6	96.4	36.8	49.6
	✓	57.6	81.6	98.6	36.8	50.4
✓	✓	38.2	62.8	90.8	22.2	28.4

poral awareness. We attribute this to two factors. First, Crop provides a cleaner and more tractable supervisory signal: because the source view fully contains the target view, the reconstruction target is well-defined and spatially grounded. In contrast, Time relies on temporally shifted targets and therefore introduces additional ambiguity from object motion, camera motion, and appearance change across frames. Second, the scene structure learned from Crop serves as a stronger inductive bias for understanding dynamics. This is consistent with our hypothesis that explicitly learning **what-is-where** is crucial for capturing how the scene evolves over time (i.e., **what-moves-where**).

Time + Crop. Given that Time provides temporal cues while Crop offers clear spatial grounding, one may expect that combining the two would yield a stronger supervisory signal. However, Tab. 3 shows that Time+Crop performs worse than both individual formulations. We conjecture that this degradation stems from a conflict between the two source-to-target relationships. When combined, the model must simultaneously resolve spatial localization and temporal change, making the target more ambiguous and reducing the quality of the supervisory signal. This further supports our use of Crop-based global-to-local formulation.

4. Related Work

Self-supervised Learning (SSL) aims to learn rich and transferable visual representations from unlabeled images or videos. A large body of SSL methods build on representation alignment across augmented views, using contrastive objectives [4, 6, 8, 16, 31] or teacher-student self-distillation [5, 13, 28, 33] to learn invariant features. Meanwhile, reconstruction-based approaches learn representations by recovering masked pixels or tokens [2, 17, 32, 33]. Despite their success, most SSL methods have primarily been evaluated on traditional tasks such as image classification and segmentation, leaving transferable representation for dynamic scene understanding largely underexplored.

Siamese Masked Autoencoder [15], on the other hand, targets dynamic scene understanding by learning visual correspondence from videos. It employs a Siamese encoder [3] to

predict masked patches in one frame from another, thereby learning patch-wise correspondence across time. CropMAE [11] further shows that similar correspondence can be learned even from static images by reconstructing one cropped view from another. However, their patch-wise correspondence learning is suboptimal for downstream video understanding tasks that require a *single* compact frame representation, such as robotic manipulation.

State Representation Learning (SRL), as introduced by ToBo [25], addresses the above limitation by learning to encode an observation into a single compact visual state (i.e., the bottleneck token). It learns this state by reconstructing heavily masked target patches from the bottleneck token of a temporally adjacent frame and a few visible target patches. This encourages temporal relationships to be preserved in the representation, but does not explicitly account for within-frame spatial structure and scene composition.

Our work extends this line of work by studying a *dynamics-aware* SSL method for learning state representations that capture scene composition. Like prior works, we use a Siamese network to process paired views and learn from their relationship through image reconstruction [11, 15, 25]. However, our work differs in two key aspects. First, we identify that compact visual state representations for dynamic world understanding should preserve scene composition. Second, to achieve this, we propose a novel global-to-local reconstruction framework that learns to encode scene composition into the bottleneck token.

5. Conclusion

Effective dynamic scene understanding of video data requires visual state representations that explicitly encode the semantic identities and precise spatial locations of scene elements in a unified manner. To this end, we introduce CroBo, a framework built around a global-to-local reconstruction objective, where a compact bottleneck token reconstructs masked local crops. Reconstruction analyses show that CroBo captures fine-grained **what-is-where** scene composition, and perceptual straightness evaluations further indicate that this spatial grounding enables representations to track **what-moves-where** across dynamic observations. Consequently, compact visual representations that preserve pixel-level scene information lead to state-of-the-art performance on vision-based robot policy learning benchmarks.

References

- [1] Piyush Bagad and Andrew Zisserman. Chirality in action: Time-aware video representation learning by latent straightening. *arXiv preprint arXiv:2509.08502*, 2025. 6, 7
- [2] Hangbo Bao, Li Dong, Songhao Piao, and Furu Wei. Beit: Bert pre-training of image transformers. *arXiv preprint arXiv:2106.08254*, 2021. 8

- [3] Jane Bromley, Isabelle Guyon, Yann LeCun, Eduard Säckinger, and Roopak Shah. Signature verification using a” siamese” time delay neural network. *Advances in neural information processing systems*, 6, 1993. 3, 8
- [4] Mathilde Caron, Ishan Misra, Julien Mairal, Priya Goyal, Piotr Bojanowski, and Armand Joulin. Unsupervised learning of visual features by contrasting cluster assignments. *Advances in neural information processing systems*, 33:9912–9924, 2020. 8
- [5] Mathilde Caron, Hugo Touvron, Ishan Misra, Hervé Jégou, Julien Mairal, Piotr Bojanowski, and Armand Joulin. Emerging properties in self-supervised vision transformers. In *Proceedings of the IEEE/CVF international conference on computer vision*, pages 9650–9660, 2021. 1, 4, 5, 8
- [6] Ting Chen, Simon Kornblith, Mohammad Norouzi, and Geoffrey Hinton. A simple framework for contrastive learning of visual representations. In *International conference on machine learning*, pages 1597–1607. PmlR, 2020. 8
- [7] Xinlei Chen, Haoqi Fan, Ross Girshick, and Kaiming He. Improved baselines with momentum contrastive learning. *arXiv preprint arXiv:2003.04297*, 2020. 1
- [8] Xinlei Chen, Saining Xie, and Kaiming He. An empirical study of training self-supervised vision transformers. In *Proceedings of the IEEE/CVF international conference on computer vision*, pages 9640–9649, 2021. 1, 8
- [9] Alexey Dosovitskiy, Lucas Beyer, Alexander Kolesnikov, Dirk Weissenborn, Xiaohua Zhai, Thomas Unterthiner, Mostafa Dehghani, Matthias Minderer, Georg Heigold, Sylvain Gelly, et al. An Image is Worth 16x16 Words: Transformers for Image Recognition at Scale. In *ICLR*, 2021. 4
- [10] Ayoub Echchahed and Pablo Samuel Castro. A survey of state representation learning for deep reinforcement learning. *arXiv preprint arXiv:2506.17518*, 2025. 1
- [11] Alexandre Eymaël, Renaud Vandeghen, Anthony Cioppa, Silvio Giancola, Bernard Ghanem, and Marc Van Droogenbroeck. Efficient image pre-training with siamese cropped masked autoencoders. In *European Conference on Computer Vision*, pages 348–366. Springer, 2024. 3, 4, 5, 7, 8
- [12] Christoph Feichtenhofer, Yanghao Li, Kaiming He, et al. Masked autoencoders as spatiotemporal learners. *Advances in neural information processing systems*, 35:35946–35958, 2022. 4
- [13] Jean-Bastien Grill, Florian Strub, Florent Altché, Corentin Tallec, Pierre Richemond, Elena Buchatskaya, Carl Doersch, Bernardo Avila Pires, Zhaohan Guo, Mohammad Gheshlaghi Azar, et al. Bootstrap your own latent—a new approach to self-supervised learning. *Advances in neural information processing systems*, 33:21271–21284, 2020. 8
- [14] Abhishek Gupta, Vikash Kumar, Corey Lynch, Sergey Levine, and Karol Hausman. Relay policy learning: Solving long-horizon tasks via imitation and reinforcement learning. *arXiv preprint arXiv:1910.11956*, 2019. 4, 5, 6, 11, 12
- [15] Agrim Gupta, Jiajun Wu, Jia Deng, and Fei-Fei Li. Siamese masked autoencoders. *Advances in Neural Information Processing Systems*, 36:40676–40693, 2023. 3, 4, 5, 7, 8
- [16] Kaiming He, Haoqi Fan, Yuxin Wu, Saining Xie, and Ross Girshick. Momentum contrast for unsupervised visual representation learning. In *Proceedings of the IEEE/CVF conference on computer vision and pattern recognition*, pages 9729–9738, 2020. 1, 8
- [17] Kaiming He, Xinlei Chen, Saining Xie, Yanghao Li, Piotr Dollár, and Ross Girshick. Masked autoencoders are scalable vision learners. In *Proceedings of the IEEE/CVF conference on computer vision and pattern recognition*, pages 16000–16009, 2022. 1, 3, 4, 5, 8
- [18] Olivier J Hénaff, Robbe LT Goris, and Eero P Simoncelli. Perceptual straightening of natural videos. *Nature neuroscience*, 22(6):984–991, 2019. 6, 7
- [19] Olivier J Hénaff, Yoon Bai, Julie A Charlton, Ian Nauhaus, Eero P Simoncelli, and Robbe LT Goris. Primary visual cortex straightens natural video trajectories. *Nature communications*, 12(1):5982, 2021. 6
- [20] Elad Hoffer, Tal Ben-Nun, Itay Hubara, Niv Giladi, Torsten Hoeffler, and Daniel Soudry. Augment your batch: Improving generalization through instance repetition. In *Proceedings of the IEEE/CVF Conference on Computer Vision and Pattern Recognition*, pages 8129–8138, 2020. 4
- [21] Christian Internò, Robert Geirhos, Markus Olhofer, Sunny Liu, Barbara Hammer, and David Klindt. Ai-generated video detection via perceptual straightening. *arXiv preprint arXiv:2507.00583*, 2025. 7
- [22] Huiwon Jang, Dongyoung Kim, Junsu Kim, Jinwoo Shin, Pieter Abbeel, and Younggyo Seo. Visual Representation Learning with Stochastic Frame Prediction. In *International Conference on Machine Learning*, pages 21289–21305. PMLR, 2024. 3, 4, 5
- [23] Justin Johnson, Bharath Hariharan, Laurens Van Der Maaten, Li Fei-Fei, C Lawrence Zitnick, and Ross Girshick. Clevr: A diagnostic dataset for compositional language and elementary visual reasoning. In *Proceedings of the IEEE conference on computer vision and pattern recognition*, pages 2901–2910, 2017. 5, 6, 11
- [24] Will Kay, Joao Carreira, Karen Simonyan, Brian Zhang, Chloe Hillier, Sudheendra Vijayanarasimhan, Fabio Viola, Tim Green, Trevor Back, Paul Natsev, et al. The kinetics human action video dataset. *arXiv preprint arXiv:1705.06950*, 2017. 4, 5
- [25] Taekyung Kim, Dongyoon Han, Byeongho Heo, Jeongeun Park, and Sangdoon Yun. Token bottleneck: One token to remember dynamics. *arXiv preprint arXiv:2507.06543*, 2025. 1, 2, 3, 4, 5, 8
- [26] Ilya Loshchilov and Frank Hutter. Decoupled weight decay regularization. *arXiv preprint arXiv:1711.05101*, 2017. 4
- [27] Xueyan Niu, Cristina Savin, and Eero P Simoncelli. Learning predictable and robust neural representations by straightening image sequences. *Advances in Neural Information Processing Systems*, 37:40316–40335, 2024. 6
- [28] Maxime Oquab, Timothée Darcet, Théo Moutakanni, Huy Vo, Marc Szafraniec, Vasil Khalidov, Pierre Fernandez, Daniel Haziza, Francisco Massa, Alaaeldin El-Nouby, et al. Dinov2: Learning robust visual features without supervision. *arXiv preprint arXiv:2304.07193*, 2023. 1, 4, 5, 8
- [29] Jordi Pont-Tuset, Federico Perazzi, Sergi Caelles, Pablo Arbeláez, Alex Sorkine-Hornung, and Luc Van Gool. The 2017

- davis challenge on video object segmentation. *arXiv preprint arXiv:1704.00675*, 2017. [5](#), [6](#), [7](#), [11](#), [12](#)
- [30] Yuval Tassa, Yotam Doron, Alistair Muldal, Tom Erez, Yazhe Li, Diego de Las Casas, David Budden, Abbas Abdolmaleki, Josh Merel, Andrew Lefrancq, et al. Deepmind control suite. *arXiv preprint arXiv:1801.00690*, 2018. [4](#), [5](#)
- [31] Zhirong Wu, Yuanjun Xiong, Stella X Yu, and Dahua Lin. Unsupervised feature learning via non-parametric instance discrimination. In *Proceedings of the IEEE conference on computer vision and pattern recognition*, pages 3733–3742, 2018. [8](#)
- [32] Zhenda Xie, Zheng Zhang, Yue Cao, Yutong Lin, Jianmin Bao, Zhuliang Yao, Qi Dai, and Han Hu. Simmim: A simple framework for masked image modeling. In *Proceedings of the IEEE/CVF conference on computer vision and pattern recognition*, pages 9653–9663, 2022. [8](#)
- [33] Jinghao Zhou, Chen Wei, Huiyu Wang, Wei Shen, Cihang Xie, Alan Yuille, and Tao Kong. ibot: Image bert pre-training with online tokenizer. *arXiv preprint arXiv:2111.07832*, 2021. [8](#)

Pixel-level Scene Understanding in One Token: Visual States Need What-is-Where Composition

Supplementary Material

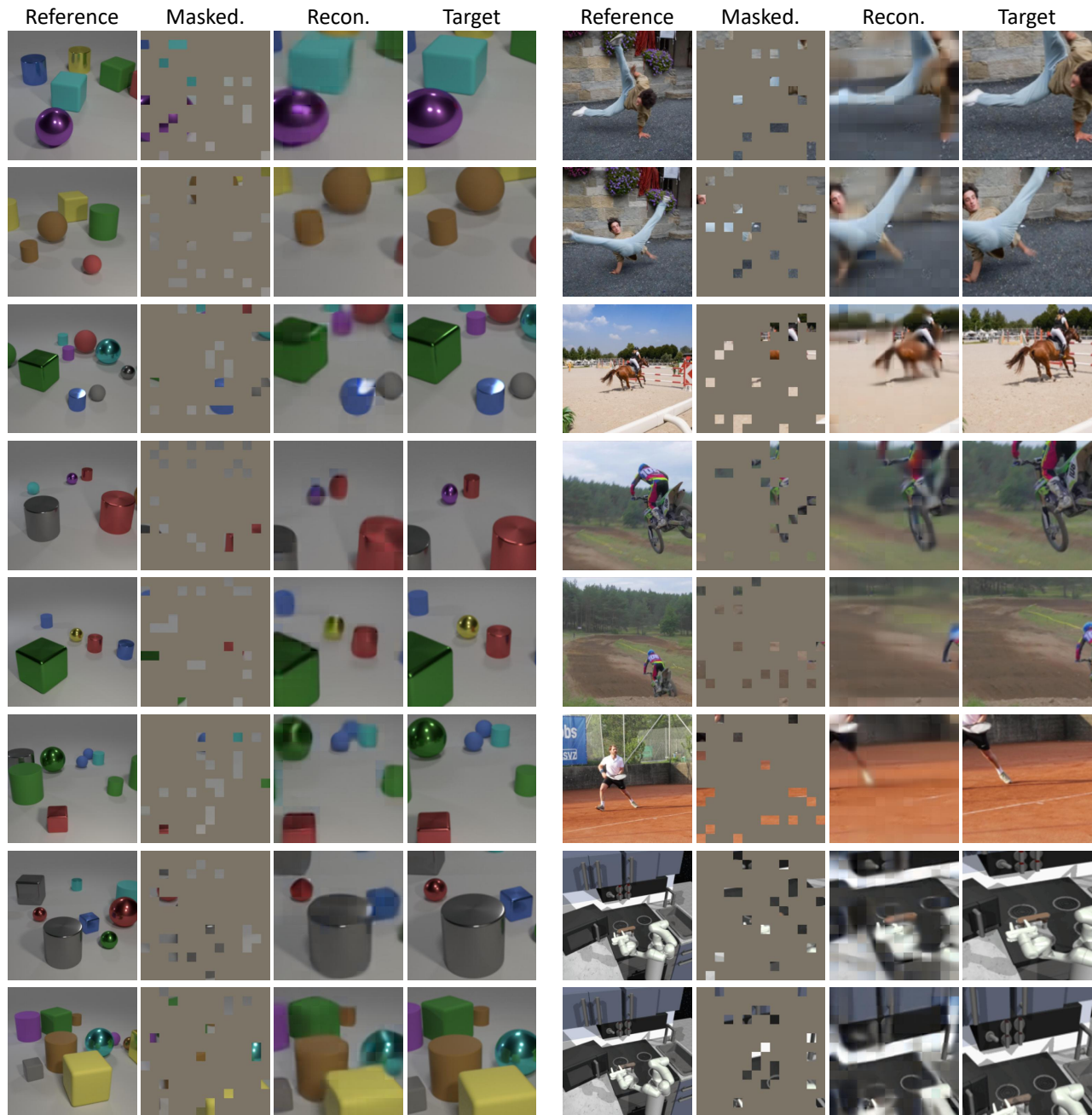


Figure 6. **Reconstruction results of CroBo.** We present image reconstruction examples on CLEVR [23], DAVIS [29], and Franka Kitchen [14]. Given the bottleneck token extracted from the source view as context, CroBo reconstructs a heavily masked (90%) target view that is spatially cropped from the source view. These reconstructions indicate that CroBo representations capture the global scene structure, including object identities, spatial locations, and their relationships.

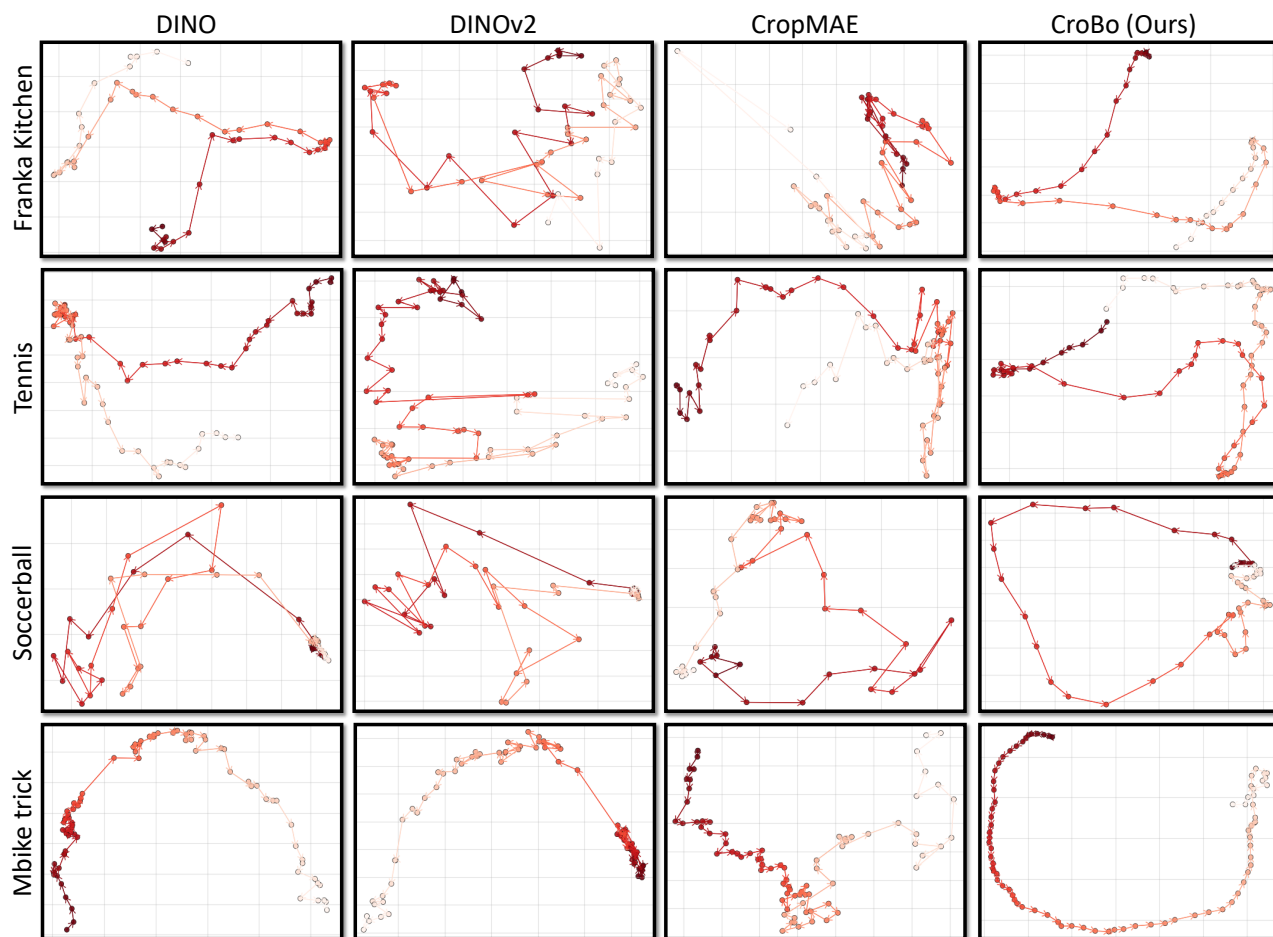


Figure 7. **Perceptual straightness of representation trajectories in video.** We visualize representation trajectories across video frames using PCA, where each point denotes a frame and colors indicate temporal order. CroBo produces smooth and locally linear trajectories that follow the natural evolution of the scene, whereas DINO, DINOv2, and CropMAE exhibit more irregular and entangled trajectories. Videos are drawn from Franka Kitchen (first row) [14] and DAVIS (remaining rows) [29].